

https://doi.org/10.1070/QEL16312

Effect of a prepulse on the efficiency of gamma-ray generation by a relativistic laser pulse obliquely incident on a planar target

D.A. Serebryakov, E.N. Nerush

Abstract. **This paper examines the effect of a density gradient produced in a target by a prepulse on the efficiency of synchrotron gamma-ray generation by a laser pulse with an intensity of the order of 10^{22} to 10^{23} W cm^{-2} obliquely incident on a planar target. We demonstrate that the gamma-ray and hard X-ray generation efficiency and the fraction of absorbed laser pulse energy can exceed those in the case of a uniform target with a sharp boundary by a factor of 1.3–2, depending on the angle of incidence. At a moderately large preplasma size, the optimal angle of incidence is 30°. At a sufficiently large size, normal incidence is optimal.**

Keywords: *laser–plasma interaction, gamma-ray generation, prepulse.*

1. Introduction

Currently, gamma-ray and hard X-ray sources are widely used in a variety of areas: from medicine to nuclear physics. Such sources utilise radioactive decay of isotopes, bremsstrahlung resulting from the scattering of relativistic electrons by nuclei [1], synchrotron radiation from electrons in a magnetic field [2] and inverse Compton scattering of laser light by relativistic electron beams produced in accelerators [3]. Progress in laser technologies and laser–plasma electron acceleration techniques allows one to avoid the use of conventional electron accelerators and create an all-optical Compton source of high-energy photons [4] or a laser–plasma betatron source [5].

In addition, a great deal of attention has recently been paid to gamma-ray and hard X-ray sources based on the interaction of laser pulses with solid targets. They became feasible with the advent of ultrahigh-power lasers whose output intensity has already reached 10^{22} W cm^{-2}, and even higher power laser systems, with expected intensities of the order of 10^{23} W cm^{-2}, are planned to be put into operation in the very near future [6, 7]. Interacting with matter, electromagnetic radiation with such intensities almost completely ionises it. At typical densities of solid targets, a laser pulse is, as a rule, predominantly reflected from the plasma surface, and high-order laser harmonics can be efficiently generated on the target surface through the following mechanisms: coherent wake emission (at nonrelativistic laser field intensities) [8] and a relativistically oscillating mirror [9, 10]. As a result, attosecond pulses can be generated on the plasma surface [11]. The maximum order of harmonics thus generated is limited by the minimum thickness of the emitting electron layer, which ensures a maximum harmonic energy of several kiloelectron volts.

At the same time, in addition to the generation of high harmonics (of coherent radiation), sufficiently high laser field intensities (of the order of 10^{22} to 10^{23} W cm^{-2}) lead to significant generation of incoherent synchrotron radiation with photon energies from hundreds of kiloelectron volts to several megaelectron volts. The synchrotron radiation power is proportional to the fourth power of the Lorentz factor of a moving electron [12], so with increasing field intensity and, hence, electron energy, an ever-larger fraction of the laser energy converts into X- and gamma-rays [13, 14]. The high-energy photon generation efficiency is influenced by not only the laser light intensity but also target parameters (density, geometric dimensions, material and others).

One key parameter influencing the interaction process is the shape of the plasma–vacuum interface. Solid targets are, as a rule, taken to have a sharp boundary, but under real experimental conditions even a weak prepulse can produce some density gradient near the interface. Using numerical simulation techniques at laser light intensities of the order of 10^{22} to 10^{23} W cm^{-2}, Nakamura et al. [15] showed that the presence of a region with an electron density gradient and a characteristic thickness of the order of a few microns can improve gamma-ray generation efficiency. In this paper, we analyse in detail the effect of density inhomogeneities on high-energy photon emission in the cases of normal and oblique incidences of a laser pulse.

2. Description of the interaction process

Characteristics of relativistic laser–plasma interaction are known to depend strongly on the relationship between the electron density in the plasma, n_e, and the dimensionless laser field amplitude $a_0 = eE/(mc\omega)$, where $\omega = 2\pi c/\lambda$ is the centre frequency of the field; c is the speed of light; and m and $e > 0$ are the electron mass and charge, respectively. A characteristic electron density demarcating different interaction regimes is the $n_{cr\,rel}$, which is a factor of a_0 higher than the critical density in a linear approximation: $n_{cr} = m\omega^2/(4\pi e^2)$. If the electron density exceeds the relativistic critical density, the plasma is opaque to a laser pulse, and it is predominantly reflected. Otherwise, the pulse penetrates into the bulk of the target and is strongly absorbed at a sufficient target thickness. This criterion is approximate: it builds on the fact that the mass of a relativistic electron exceeds the electron rest mass by a factor

D.A. Serebryakov, E.N. Nerush Institute of Applied Physics, Russian Academy of Sciences, ul. Ul'yanova 46, 603950 Nizhnii Novgorod, Russia; e-mail: dms@appl.sci-nnov.ru

Received 6 February 2017
Kvantovaya Elektronika **47** (3) 206–211 (2017)
Translated by O.M. Tsarev

of γ (where $\gamma = 1/\sqrt{1 - v^2/c^2}$ is the relativistic Lorentz factor of an electron), which is typically of the order of a_0 for $a_0 \gg 1$. Most of the absorbed energy goes into heating electrons, which then emit synchrotron X-rays. The ions have no time to gain considerable energy on a femtosecond timescale, so their dynamics typically have no qualitative effect on the interaction process. Thus, to maximise the gamma-ray energy yield, a laser pulse should be absorbed as strongly as possible. To this end, one should use targets with an electron density no higher than the relativistic critical one, because otherwise the gamma-ray generation efficiency will be much lower [16].

In most solids, the electron density in the case of complete ionisation lies in the range $(150-1000)n_{cr}$. Consequently, to maximise laser pulse absorption in a solid target, a laser pulse with $a_0 > 150$ is needed. There are currently no such lasers (but this threshold is anticipated to be overcome in the next decade in ELI facilities [17]). Therefore, to raise the gamma-ray generation efficiency, the electron density in the plasma should be reduced. One approach aimed at achieving this is to use structured targets, such as aerogels and nanowires. Owing to inhomogeneities in targets, the density of the resulting plasma can be tens and hundreds of times lower than that of the solid target material. Such targets are, however, rather difficult to produce, and density inhomogeneities can qualitatively change the interaction process.

Another approach to reducing the electron density in a plasma is to produce an electron density gradient near the target surface. When a solid target is exposed to a laser pulse, a gradient often appears in a natural way, due to the prepulse. In laser physics, a prepulse is usually thought to be a parasitic effect, which should be avoided, but in some instances it can play a positive role. Having a considerably lower intensity than the main pulse, a prepulse heats up and partially ionizes the material near the target surface. At the instant when the main pulse arrives, the heated plasma may be distributed in space over a region up to several tens of microns from the initial position of the target surface.

The efficiency of laser pulse absorption in a plasma (and, hence, that of X- and gamma-ray generation) can be improved not only by optimising the electron density but also by using obliquely incident p-polarised laser pulses. This approach allows gamma-ray generation efficiency to be raised by about a factor of 1.5 [18]. It is of interest to examine how the X- and gamma-ray generation efficiency and laser energy absorption respond to a combination of an oblique laser pulse incidence and a plasma density gradient at laser light intensities of the order of 10^{22} to 10^{23} W cm^{-2}. This issue is addressed in this paper.

3. Numerical simulation

A laser pulse penetrating a plasma layer with a density gradient experiences relativistic self-focusing, which leads to channelling of the pulse. As a result, the field intensity at the leading edge of the laser pulse increases and the electron density decreases due to the effective ponderomotive force acting on the electrons. This also influences the high-energy photon generation efficiency. For this reason, a detailed analysis of the process requires the use of numerical simulation techniques even in the case of normal incidence of laser pulses.

As shown by Nakamura et al. [15], in the case of normal incidence a density gradient drastically increases the generated gamma-ray power. The optimal size of electron density inhomogeneities, which ensured the highest gamma-ray power, was about 10 to 15 laser wavelengths. However, even when the thickness of the layer with a density gradient was a few laser wavelengths, it ensured a marked increase in laser pulse absorption and high-energy photon generation efficiency.

To simulate the interaction of relativistic laser radiation with matter, we used a three-dimensional code [19] implementing the particle-in-cell (PIC) method. The code includes a module describing high-energy photon emission using the Monte Carlo method (gamma-ray and hard X-ray photons whose wavelengths are much smaller than the grid size are treated as quasiparticles). The photon emission probability is described by quantum-electrodynamic formulas (see the 'alternative' method in Elkina et al. [20]), which allows laser–plasma interaction to be simulated with good accuracy in a very wide range of laser field intensities (up to $a_0 \approx 10000$). The high-energy photon generation process is taken to be completely incoherent, because the characteristic synchrotron radiation frequencies, $\omega_{sync} \approx c\gamma^3/R$ (where R is the local radius of curvature of the electron trajectory), in the problem under consideration lie in the range corresponding to energies from tens of kiloelectron volts to several megaelectron volts, and the emitted photon wavelengths are much shorter than the spacing between the emitters (which are randomly distributed in space). The key features of the code were described in greater detail elsewhere [14, Section 2].

In our numerical simulations, the target had the form of a 4-μm-thick plasma layer with constant electron and ion densities (in one case) or electron and ion densities linearly increasing along the x coordinate (in the other case) (the target was parallel to the yz plane). In the latter case, the target thickness x_g was 4 or 8 μm. In the case of the uniform plasma, the electron density was 40% to 80% of the relativistic critical density. As shown earlier [18, 21], it is in this density range that gamma-rays are emitted most efficiently. In the case of the targets with a density gradient, the maximum density was $0.9_{cr\,rel}$. This was found to be sufficient for a laser pulse to be almost completely absorbed in the target. Further raising the maximum density in numerical simulations is unreasonable because this only causes the point where the electron density is of the order of the relativistic critical density and around which effective reflection occurs to shift to the left.

In the first series of numerical experiments, the peak laser pulse intensity was 8.3×10^{21} W cm^{-2} (amplitude $a_0 = 55$). Such intensity has been reached to date in many petawatt laser facilities all over the world [22]. The laser pulse was p-polarised with a $\cos^2(\pi x/2\sigma_{x,r})$ envelope ($2\sigma_x$ and $2\sigma_r$ are the pulse length and cross-sectional size, respectively), which is a spatially limited Gaussian envelope approximation. The laser pulse beam radius σ_r was 3 μm and the pulse duration was 30 fs ($\sigma_x = 4.5$ μm). The centre laser wavelength was $\lambda = 1$ μm. The angle of incidence of the laser pulse was 0, 18°, 30° or 45°. The spatial grid size in our numerical simulations was 0.015λ along the x coordinate and 0.1λ along the transverse coordinate (the NDFX algorithm for solving Maxwell's equations [23] takes the x axis to be a preferential direction), and the number of particles per cell was two (test simulations with a smaller grid size and a larger number of particles per cell showed no significant distinctions between results). Figure 1 shows the electromagnetic field energy density, electron density, and high-energy photon density distributions obtained in

numerical simulations for $\theta = 30°$ and $x_g = 4\lambda$ at different instants of time t.

The energy characteristics derived from the simulation are the maximum laser field energy absorption coefficient,

$$\mu = \frac{W_{abs}}{W_0} = \frac{W_{field}\big|_{t=0} - \min\limits_t W_{field}}{W_{field}\big|_{t=0}}, \quad (1)$$

and high-energy photon generation efficiency,

$$\eta = \frac{W_{ph}}{W_0} = \frac{\sum \hbar\omega_X\big|_{t=t_{end}}}{W_{field}\big|_{t=0}}, \quad (2)$$

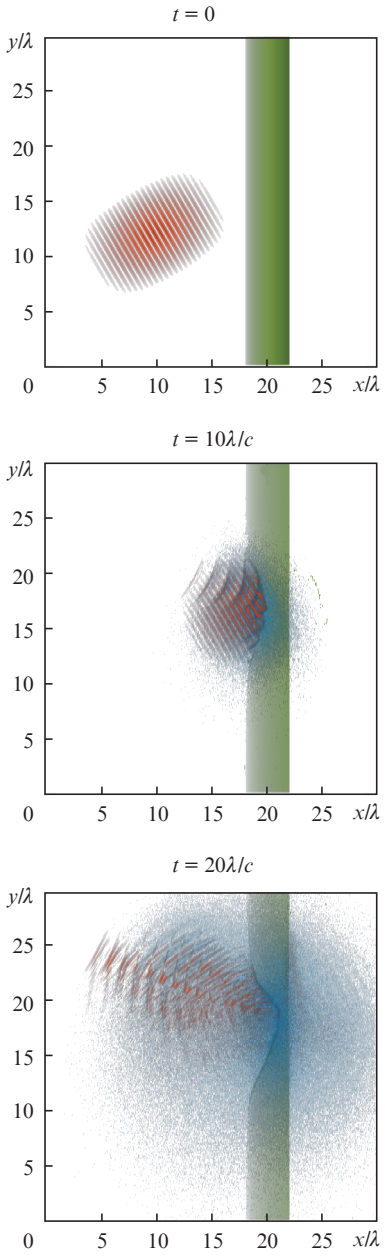

Figure 1. (Colour online) Numerical three-dimensional PIC simulation results for oblique incidence of a laser pulse at $a_0 = 55$ on a plasma layer having a density gradient: electromagnetic field energy density (red colour), electron density (green colour), and high-energy photon density (blue colour) distributions.

where W_{field} is the total energy of 'low-frequency' electromagnetic fields (described numerically as waves) in the simulation region; ω_X is the frequency of the high-energy photon obtained by the Monte Carlo method; and t_{end} is the instant at which the simulation was ended. The definitions of μ and η differ because the high-energy photon energy is an essentially monotonic function of time (at the parameters under consideration, the probability of photon absorption by electrons is negligible). The electromagnetic field energy is a nonmonotonic function of time: as a rule, its minimum coincides with the instant at which the laser light penetrates the plasma to the maximum depth. It should be noted that one often considers the laser light absorption coefficient defined as the ratio of the absorbed energy to the total energy of the radiation at the end of the simulation. The use of this parameter is more justified from an experimental point of view, but to accurately determine it, the simulation time and region should be increased. Because of this, we think it is possible to measure μ and draw conclusions from the results as to the laser light absorption.

Figure 2 shows the laser field absorption coefficient μ and high-energy photon generation efficiency η as functions of the angle of incidence θ. The data were obtained for both a target with a density gradient ($x_g = 4\lambda$ and 8λ) and a target uniform in electron density (densities of $20n_{cr}$ and $40n_{cr}$, which corresponds to $0.36n_{cr\,rel}$ and $0.72n_{cr\,rel}$, respectively). It can be seen that the presence of a preplasma markedly improves both the laser pulse absorption efficiency and the X- and gamma-ray generation efficiency. Note that a smoother density profile corresponds to higher efficiency.

The dependences of μ and η on the angle θ of incidence proved to be nontrivial. For a plasma with no density gradient and with a 4-μm-thick gradient layer, increasing the angle of incidence to 30° leads to an increase in absorption and high-energy photon generation efficiency. The optimal angle of incidence, $\theta = 30°$, agrees with that obtained previously [18, 24]. Further increasing θ reduces the efficiency. In contrast, at $x_g = 8$ μm the optimal geometry is normal incidence ($\theta = 0$), whereas at oblique incidence the efficiency is slightly lower. On the whole, it is worth noting that a density gradient increases the absorption efficiency by about 30% to 50%.

The following physical mechanisms may be responsible for the different $\mu(\theta)$ and $\eta(\theta)$ dependences in the cases of sharp and smooth density profiles. At oblique incidence of a p-polarised pulse on a sharp plasma boundary, the increase in absorption efficiency is due to the presence of a laser light electric field component normal to the surface, E_x, which leads to electron 'ejection' from the target surface and more efficient interaction of the electrons with the laser field [25]. If the gradient is small (and, hence, the density profile is smooth), the contribution of this effect decreases. As a result, oblique incidence is no longer more advantageous than normal incidence. Note, however, that understanding exact causes of the change in $\mu(\theta)$ and $\eta(\theta)$ behaviours requires a more detailed analysis.

A similar series of numerical simulations was performed as well for a laser pulse with an amplitude increased by a factor of 4 ($a_0 = 220$, $I = 1.33\times10^{23}$ W cm^{-2}) and a proportionally increased electron density in the target (according to similarity laws [26], this has no effect on laser–plasma interaction). The simulation results [$\mu(\theta)$ and $\eta(\theta)$ dependences] are presented in Fig. 3. Like at $a_0 = 55$, the absorption coefficient and gamma-ray generation efficiency increase, and the increase in efficiency at $a_0 = 220$ is even larger: the effi-

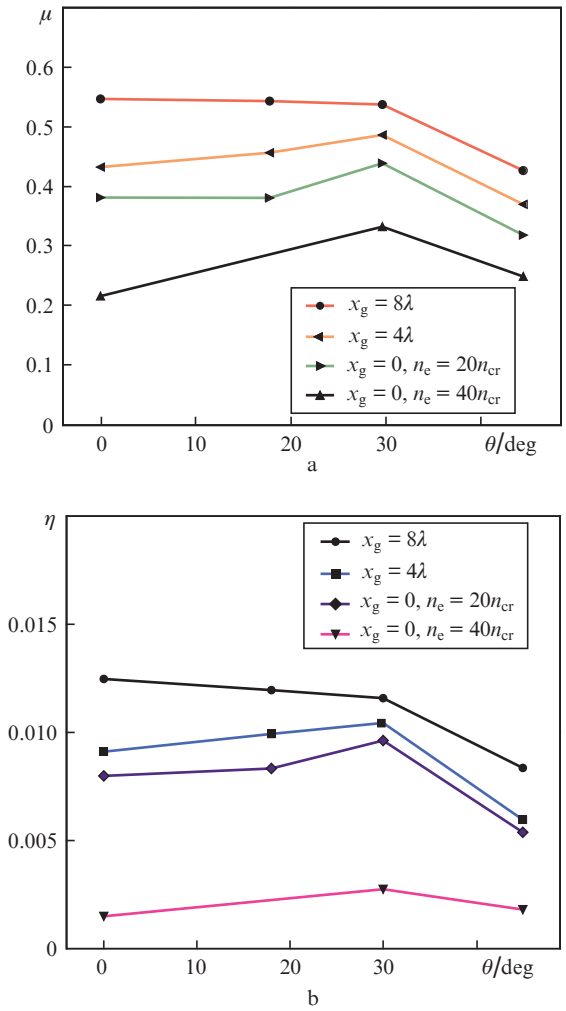

Figure 2. (a) Fraction of absorbed laser pulse energy, μ, and (b) high-energy photon generation efficiency, η, as functions of the angle of incidence of a p-polarised laser pulse at $a_0 = 55$. The electron density in the target varies linearly from 0 to $50n_{cr}$ with x_g or is constant (at $x_g = 0$).

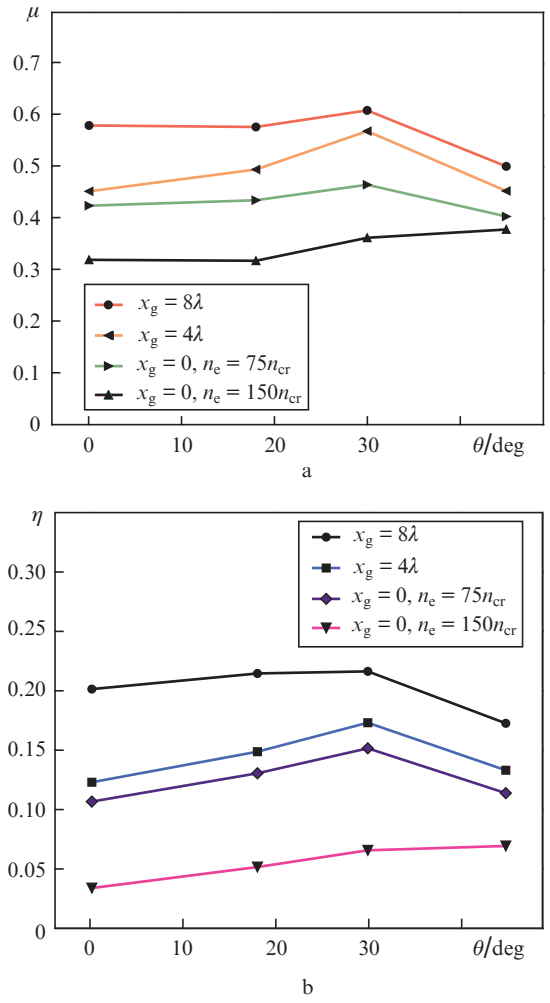

Figure 3. (a) Fraction of absorbed laser pulse energy, μ, and (b) gamma-ray generation efficiency, η, as functions of the angle of incidence of a p-polarised laser pulse at $a_0 = 220$. The electron density in the target varies linearly from 0 to $200n_c$ with x_g or is constant (at $x_g = 0$).

ciency increases by a factor of 1.5–2 (compared to the target without a preplasma). It can also be seen that there is no monotonic decrease in efficiency with increasing θ at a smooth density profile, but the difference between the efficiencies at different angles is not very large. One possible reason for this is that the magnitude of the gradient dn_e/dx is a factor of 4 smaller than that in the analogous simulations at $a_0 = 55$. It seems likely that, further increasing x_g to several tens of laser wavelengths, we would also observe a change in $\mu(\theta)$ and $\eta(\theta)$ behaviours, but the corresponding simulations would require several times more computational power, more memory, etc. We plan to examine this case in greater detail in the future.

When an ultra-intense laser pulse interacts with a plasma, the synchrotron radiation almost always generates a wide spectrum of high-energy photons. Figure 4 shows X- and gamma-ray spectra at $a_0 = 55$ and 220. They are typical synchrotron radiation spectra, with a rather broad maximum at low energies (of the order of tens of kiloelectron volts at $a_0 = 55$ and of the order of hundreds of kiloelectron volts to several megaelectron volts at $a_0 = 220$) and a rather rapid decrease at higher energies. Thus, placing a boundary between X- and gamma-rays at 100 keV, we can see that a considerable fraction of the synchrotron radiation energy at $a_0 = 55$ or most of it at $a_0 = 220$ lies in the gamma-ray region. It should be noted that the shape of the spectrum is essentially independent of whether the plasma is uniform or not. Gamma-ray and hard X-ray sources having a wide spectrum can be useful in a variety of applications, e.g. in radioactive isotope detection, flaw detection, etc.

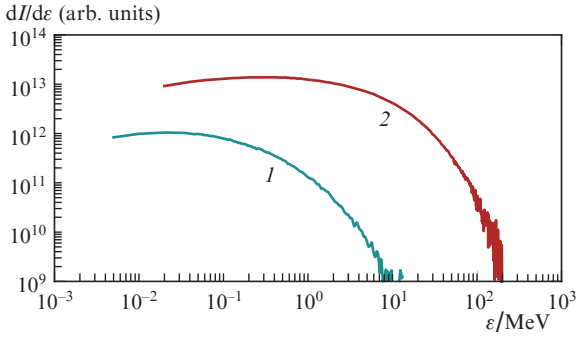

Figure 4. Typical high-energy photon spectra obtained in numerical simulations at $a_0 = (1)$ 55 and (2) 220.

It is also of interest to analyse how gamma-radiation patterns are influenced by an electron density gradient. Figure 5 shows radiation patterns in the xy plane (coinciding with the plane of polarisation of the laser pulse) at normal and oblique ($\theta = 30°$) incidence. It is seen that an electron density gradient has a weak effect on the shape of the radiation pattern, which is determined primarily by the angle of incidence of the laser pulse. At normal incidence, the radiation pattern is symmetric. At oblique incidence, we observe a main maximum, in a direction roughly corresponding to the pulse reflection direction, and a side maximum, along the x axis (normal to the surface). Note that the gamma-rays form rather narrow beams: their angular width is about 20° to 30° (the angular spread of a photon pulse along the z axis, not shown in Fig. 5, also does not exceed 20° to 30°), which makes this regime more attractive for potential practical applications.

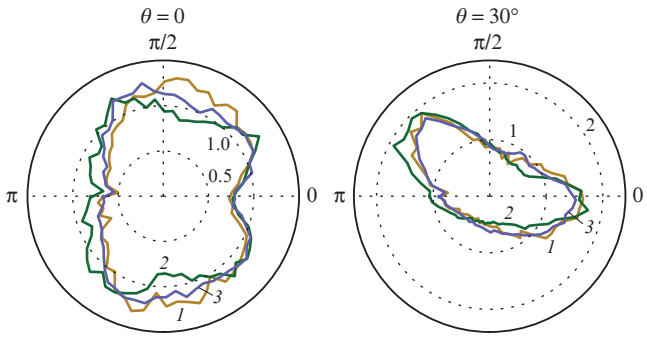

Figure 5. Gamma-radiation patterns in the plane of polarisation of a laser pulse at $a_0 = 220$ for normal and oblique ($\theta = 30°$) incidence at $x_g =$ (*1*) 0, (*2*) 4, and (*3*) 8 μm. Each value in the patterns (at angles from 0 to 2π) is the ratio of the energy emitted in a given direction to that for isotropic radiation (the contour lines of this ratio are shown by dashed circles).

4. Conclusions

The present simulation results highlight that, in analysing the generation of gamma-ray and hard X-rays through the interaction of laser light of intensity of the order of 10^{22} to 10^{23} W cm^{-2} with solid targets, it is important to take into account plasma density inhomogeneities. In agreement with previously reported results [15], we have demonstrated that an electron density gradient in a plasma improves the synchrotron radiation generation efficiency. At the same time, the most important result of this study is that we have determined the laser energy absorption efficiency and high-energy photon generation efficiency as functions of the angle of incidence of laser radiation at the intensities in question. In particular, it has been shown that, at a sharp electron density profile, the optimal angle of incidence of a p-polarised pulse is $\theta = 30°$ (as in the case of a sharp plasma boundary) and that, at a smoother profile, normal incidence may be more attractive from the viewpoint of high-energy photon generation efficiency. It seems likely that the nature of the dependence changes because the Brunel mechanism [25], responsible for the increase in generation efficiency at oblique incidence on a sharp plasma boundary, becomes inoperative as the size of plasma inhomogeneities increases.

Thus, a prepulse can improve the efficiency of gamma-ray generation through the interaction of laser light of intensity of the order of 10^{22} to 10^{23} W cm^{-2} with solid targets, and the angle of incidence can be optimised depending on the prepulse power and duration (which influence the electron density gradient). This is an important result, useful for possible experiments with real targets.

Acknowledgements. This work was supported by the Presidium of the Russian Academy of Sciences (Programme 'Extreme laser radiation: physics and fundamental applications') and the Russian Foundation for Basic Research (Grant No. 15-02-06079).

References

1. Wagner A., Beyer R., Erhard M., Grosse E., Hartmann A., Junghans A., Kosev K., Mallion S., Nair C., Nankov N., et al. *J. Phys. G: Nucl. Part. Phys.*, **31**, S1969 (2005).
2. Bilderback D.H., Elleaume P., Weckert E. *J. Phys. B: At. Mol. Opt. Phys.*, **38**, S773 (2005).
3. Weller H.R., Ahmed H.R., Gao H., Tornow W., Wu Y.K., Gai M., Miskimen R. *Prog. Part. Nucl. Phys.*, **62**, 257 (2009).
4. Phuoc K.T., Corde S., Thaury C., Malka V., Tafzi A., Goddet J.P., Shah R.C., Sebban S., Rousse A. *Nat. Photonics*, **6**, 308 (2012).
5. Nerush E.N., Kostyukov I.Yu. *Phys. Rev. E*, **75**, 057401 (2007).
6. Papadopoulos D., Le Blanc C., Chériaux G., Georges P., Mennerat G., Zou J.P., Mathieu F., Audebert P. *Proc. Advanced Solid State Lasers 2013 Conf.* (Paris, 2013) paper ATu3A.
7. Zamfir N.V. *EPJ Web Conf.*, **66**, 11043 (2014).
8. Quere F., Thaury C., Monot P., Dobosz S., Martin Ph. *Phys. Rev. Lett.*, **96**, 125004 (2006).
9. Bulanov S.V., Naumova N.M., Pegoraro F. *Phys. Plasmas*, **1**, 745 (1994).
10. Dromey B., Zepf M., Gopal A., Lancaster K., Wei M.S., Krushelnick K., Tatarakis M., Vakakis N., Moustaizis S., Kodam R., Tampo M., Stoeckl C., Clarke R., Habara H., Neely D., Karsch S., Norreys P. *Nat. Phys.*, **2**, 456 (2006).
11. Cherendychek M., Pukhov A. *Quantum Electron.*, **46**, 353 (2016) [*Kvantovaya Elektron.*, **46**, 353 (2016)].
12. Landau L.D., Lifshitz E.M. *The Classical Theory of Fields* (Amsterdam: Elsevier, 1975; Moscow: Nauka, 1988).
13. Ji L.L., Pukhov A., Nerush E.N., Kostyukov I.Yu., Shen B.F., Akli K.U. *Phys. Plasmas,* **21**, 023109 (2014).
14. Nerush E.N., Kostyukov I.Yu., Ji L., Pukhov A. *Phys. Plasmas*, **21**, 013109 (2014).
15. Nakamura T., Koga J.K., Esirkepov T.Zh., Kando M., Korn G., Bulanov S.V. *Phys. Rev. Lett.*, **108**, 195001 (2012).
16. Artemenko I.I., Golovanov A.A., Kostyukov I.Yu., Kukushkina T.M., Lebedev V.S., Nerush E.N., Samsonov A.S., Serebryakov D.A. *Pis'ma Zh. Eksp. Teor. Fiz.*, **104**, 892 (2016).
17. http://www.eli-laser.eu/.
18. Serebryakov D.A., Nerush E.N. *Quantum Electron.*, **46**, 299 (2016) [*Kvantovaya Elektron.*, **46**, 299 (2016)].
19. Nerush E.N., Kostyukov I.Yu. *Vopr. At. Nauki Tekh.*, **68**, 3 (2010).
20. Elkina N.V., Fedotov A.M., Kostyukov I.Yu., Legkov M.V., Narozhny N.B., Nerush E.N., Ruhl H. *Phys. Rev. ST Accel. Beams*, **14**, 054401 (2011).
21. Serebryakov D.A., Nerush E.N., Kostyukov I.Yu. *Phys. Plasmas*, **22**, 123119 (2015).

22. Danson C., Hillier D., Hopps N., Neely D. *High Power Laser Sci. Eng.*, **3**, e3 (2015).
23. Pukhov A. *J. Plasma Phys.*, **61**, 425433 (1999).
24. Pan K.Q., Zheng C.Y., Wu D., He X.T. *Phys. Plasmas*, **22**, 083301 (2015).
25. Brunel F. *Phys. Rev. Lett*., **59**, 52 (1987).
26. Gordienko S., Pukhov A. *Phys. Plasmas*, **12**, 043109 (2005).